Journal name: Ecosphere

Manuscript type: Methods, Tools, and Technologies

Evaluating camera trap methods for monitoring population trends in ungulates: insights from simulation

Clément Calenge[1] Sonia Saïd[2] Jules Chiffard[3] Mathieu Garel[4,*] Maryline Pellerin[5,*]

[1] Office Français de la Biodiversité – Direction Surveillance, Évaluation, Données – Unité Données et Appui Méthodologique, Saint Benoist, BP 20. 78612 Le Perray en Yvelines, France. ORCID: 0000-0001-7741-8016.

[2] Office Français de la Biodiversité – Direction Recherche et Appui Scientifique - Service Conservation et gestion des espèces à enjeux, Birieux, France. ORCID: 0000-0003-1485-8297.

[3] Office Français de la Biodiversité – Direction Recherche et Appui Scientifique - Service SantéAgri, Villeneuve de Rivière, France. ORCID: 0000-0002-7767-8106.

[4] Office Français de la Biodiversité – Direction Recherche et Appui Scientifique - Service Anthropisation et fonctionnement des écosystèmes terrestres, Gières, France. ORCID: 0000-0002-5978-7122.

[5] Office Français de la Biodiversité – Direction Recherche et Appui Scientifique - Service Conservation et gestion durable des espèces exploitées, Chateauvillain, France. ORCID: 0009-0008-0734-956X.

Authorship statement: * equal contribution, sorted alphabetically

Correspondence: Clément Calenge. E-mail: clement.calenge@ofb.gouv.fr

Open research: Code and data are available from Zenodo: https://doi.org/10.5281/zenodo.16989360.

Keywords: random encounter models, instantaneous sampling, simulations, animal movement, habitat selection, sampling design

Abstract

Camera traps have been widely used in the last decade to monitor abundance of unmarked animal populations. Most estimation methods rely either on the number of times animals pass through the detection zones, like random encounter models (REM) or on the number of capture occasions in a time-lapse program when animals were seen on the pictures, like the instantaneous sampling approach (IS). Yet, the ability of these two popular method classes to both reliably detect population trends and estimate population size has rarely been evaluated. We filled this gap by simulating a setup of either 100 or 25 camera traps randomly distributed on a 2600-ha area (respectively $\approx$ 4 and 1 trap/km^2), along with the movements of a fictional population of 300 roe deer (*Capreolus capreolus*). Simulations were informed by field data on habitat, habitat selection and activity patterns of GPS-monitored roe deer. Assuming perfect knowledge of key parameters (e.g., day range), constant sensor sensitivity and full correction for imperfect visibility within the detection zone, both IS and REM provided unbiased estimates of population size, but uncertainty remained substantial (CV: 15% at high trap density, up to 30% at low trap density). Moreover, despite idealized conditions and large sampling efforts, a simulated 20% population decline over 5 years went undetected by both approaches in 65-75% of simulations at high trap density and 80% at low trap density. Testing other sampling strategies to improve sensitivity either led to an unchanged population size estimation precision (stratified sampling) or to biased estimated trends (sampling only in high-quality habitats). Simulating animals with a 10 times larger home-range, like red deer (*Cervus elaphus*), led to miss the decline less frequently (5% – 40% at high trap density, 33% – 67% at low trap density). These results suggest that the key metric for camera trap use is the average number of different traps visited per animal, which in turn depends on trap density, home-range size and space use heterogeneity. We provide a R package allowing the reader to reproduce these simulations, and carry out their own.

Introduction

Camera traps are used to reach many goals in wildlife studies, including estimating occupancy, studying animal behaviour, and investigating species interactions, in particular predator-prey interactions (see the review by Burton et al., 2015). Because in some species individual identification is possible based on phenotypic patterns, estimating the size of populations with capture-recapture methods has also been among the first use of camera traps, especially in elusive carnivores (Karanth, 1995). More recently, a large amount of literature has been devoted to the use of camera traps to estimate the size of the population of non individually identifiable animals (Rowcliffe et al., 2008; Nakashima et al., 2017; Howe et al., 2017; Moeller et al., 2018). The basic idea of these methods is that the number of animals detected by the traps can be used to infer the number of animals present in the study area.

Two main families of methods have been proposed to achieve this aim: those based on animal-trap encounters, which quantify the number of animals passages through the detection zones of traps motion sensors, and those based on animal-trap associations, which count animals at capture occasions within time-lapse programs (Campos-Candela et al., 2018). The random encounter model (REM, Rowcliffe et al., 2008) is a prominent example of the first family, while camera trap distance sampling (Howe et al., 2017), instantaneous sampling (IS, Moeller et al., 2018) or the similar "association model" of Campos-Candela et al. (2018) exemplify the second.

These estimation methods are often seen as a grail, in that they allow the estimation of population abundance, a key population parameter (Williams et al., 2002) without the intensive effort of capture-recapture. This is particularly appealing to many practitioners (Gilbert et al., 2020), who often rely on less burdensome index-based methods that only allow for trend estimation (Morellet et al., 2007; Garel et al., 2010). Consequently, some even propose replacing their established monitoring methods (whether capture or index-based) with camera trap-based approaches, driven by the perception that they are

easier to implement and will facilitate both abundance and trend estimation (pers. obs.). This might be a problem, as the properties of these new methods are not yet fully understood, and numerous factors must be considered when using them (Calenge, 2025).

Thus, one major issue when estimating a population size is the imperfect detectability of the animals in the detection zone (Gilbert et al., 2020). Most camera trap studies rely on the use of motion sensors to trigger the traps when an animal enters the detection zone. However, such sensors are less sensitive when the animals are small (Glen et al., 2013) or far from the trap (Howe et al., 2017). The camera traps characteristics (brand, model, wear, etc.) may also have an effect on the detection probability of the animals in the detection zone (Palencia et al., 2021). Obstacles and environmental conditions may further limit its effective surface area (Palencia et al., 2021; Moeller et al., 2023). Numerous authors have insisted on the need to account for this imperfect detection in population size estimation (e.g., Howe et al., 2017; Moeller et al., 2023). However, most practitioners continue to ignore this issue, leading to potential biases in their estimates (Burton et al., 2015). Nevertheless, population trend estimates may still be unbiased, unless habitat structure changes over time (e.g. vegetation growth or human disturbance, Guillera-Arroita, 2017).

An issue tied to the broader problem of imperfect detection is the existence of periods during which animals are inactive and less detectable by motion sensors. Such periods do not necessarily affect estimation accuracy if the camera traps are randomly distributed over the study area, and if the resting areas have the same probability to be monitored as other areas (i.e., no refuges where the animals are undetectable, Rowcliffe et al., 2014). However, even when these assumptions are satisfied, the decreased detectability of inactive animals by motion sensors in the trap detection zone can lead to density underestimation (Corlatti et al., 2020). Numerous methods have been proposed to account for such activity patterns in population size estimation (e.g. Nakashima et al., 2017), though a common approach is to focus the monitoring on periods when it is reasonable to suppose that all

animals are active (Howe et al., 2017).

Given these potential sources of bias, the empirical validation of camera trap-based methods for estimating population size is crucial, yet remains limited. So far, most comparative studies have employed reference density values estimated using established methods such as conventional distance sampling (Rovero and Marshall, 2009; Caravaggi et al., 2016) or capture-recapture (Twining et al., 2022). However, these comparisons, carried out over a few years, often involve only a limited number of imprecise estimates from both camera-trap estimation methods and "reference" methods, often leading to conclusions that no difference can be detected between the two families of methods, which does not constitute proof of estimate equivalence. On the other hand, simulations offer a valuable alternative, enabling numerous replications of a specific camera trap study setup under fully known and user-controlled demographic and spatial conditions (Santini et al., 2022). However, so far, few studies have explored the conditions under which camera trap-based estimates may be biased or robust.

In this paper, we assess the feasibility of using camera traps to monitor roe deer (*Capreolus capreolus*) abundance over time through simulation, while examining how camera and habitat characteristics, along with animal behaviour, influence detection probabilities. Specifically, we explore how the differential use of habitats with varying detection properties, combined with the animals' activity rhythms, affects their detectability. To do so, we simulated realistic movements of animals, incorporating habitat selection and activity patterns (resting, foraging and exploring) informed from the GPS-monitoring in a roe deer population. We simulated a decreasing trend in population size across years, and a correlated increase in home-range size (Kjellander et al., 2004). We assessed the estimation precision and the ability to detect the simulated declining trend of two of the most widely classes of models for estimating population size: one based on individual encounters (random encounter model, Rowcliffe et al., 2008) and the other on associations (instantaneous sampling, Moeller et al., 2018). We also assessed the effect of

placing all camera traps in the most selected habitat type, as well as the effect of stratified sampling, on the precision of the trend estimates – two commonly used procedures when setting up camera traps in the field. Finally, we explored the possibility to expand these results to other species with a larger home range, such as red deer (*Cervus elaphus*).

We provide a companion R package named `simCTChize`, available at https://github.com/ClementCalenge/simCTChize, containing all the code and data used for these simulations (also available on Zenodo: https://doi.org/10.5281/zenodo.16989360). Appendix S1 corresponds to the package PDF vignette, and describes how the user can install this package and easily reproduce the calculations carried out in this paper. This vignette also includes numerous additional details on the simulations that we omit in this paper to keep it as concise as possible (specific values of the parameters used for the movement processes or the detection functions of the camera traps, density of trees simulated in the detection zone, etc.). Finally, this package also contains a tutorial allowing the user to design their own simulations if they want to design a monitoring for another species.

Material and Methods

Simulating realistic roe deer movements and their detection by camera traps

We first simulated a population of moving animals in the Chizé reserve, France (46.106° N, 0.424° W), during five years. We chose this enclosed 2614 ha forested study area because its roe deer population has been monitored for 50 years (Pellerin et al., 2017), and space use by the roe deer was extensively studied (Saïd et al., 2005; Pellerin et al., 2008, 2010; Gaudry et al., 2018). This population monitoring provides us with a wealth of data on demographic parameters (survival, reproductive rates, Gaillard et al., 1993), enabling the development of realistic population simulations. The northern part of the study area (1385

ha) is mainly composed of an oak stand (*Quercus* spp.) characterized by a high quality forage source, whereas the southern part (1229 ha) is mainly composed of a beech stand (*Fagus sylvatica*) with poor resource quality (Pettorelli et al., 2001). Consequently, roe deer density is higher in the northern part of the area, a spatial heterogeneity that we incorporated into our subsequent simulations.

We simulated animal movements using a model that combined multiple Ornstein-Uhlenbeck with foraging (OUf) processes (Fleming et al., 2014). Each process was characterized by distinct parameters – attraction points, speed and relocation autocorrelations, and patch sizes – to represent various animal movement behaviours, such as foraging and inter-patch movements, analogous to the mixed models proposed by Blackwell (1997) and Michelot et al. (2019). The model also accounted for the presence of resting periods.

Sets of attraction points for these OUf processes were simulated using the following approach: we first used the kernel method to estimate 25 utilization distributions using GPS data from 15 roe deer monitored in Chizé in March from 2003 to 2008 (some roe deer were monitored during multiple years; see Pellerin et al., 2008, for more details on the monitoring of these animals). We then identified the local modes of these distributions. This resulted in 25 sets of points (between 1 and 17 points per set), which we used to simulate the presence of attraction points for our simulated animals. To simulate the movement of an animal, we randomly selected one of these sets and randomly placed it on our study area, giving its centroid a probability equal to 0.64 to be located in the northern part to reflect the higher habitat quality in this region, as reported by Pettorelli et al. (2001). We made sure that all the simulated movements remained within the study area, to guarantee animal presence throughout the study and avoid edge effects on our results. When an animal survived across multiple years (see below), we used the same centroid for this animal during all years, thereby simulating its sedentarity.

We then simulated our movement model using this located set of attraction points.

Analysis of the GPS data showed that we could roughly describe animal movements as randomly switching between three behaviours: resting (immobility), patch-level movements (movement concentrated within a very small portion of the home range, generally corresponding to foraging) and between-patch movements (larger movements within the home range). Our movement model therefore simulated three behaviour types: (i) resting (the animal does not move), (ii) Patch-level movements characterized by OUf processes with small variances and centred on one attraction point (see below); (iii) Between-patch movements characterized by OUf processes with larger variances, also centred on one attraction point. Appendix S1 gives more details on the precise parameterization of these OUf processes. We used the GPS data to derive rough estimates of the daily frequency and timing of these movements types (unpublished results), which were used to parameterize the movements in our simulations.

Fig. 1 gives a schematic description of the approach used to simulate the random switching between behaviours. We simulated the same activity cycle for all animals and all days of the study period. We simulated the animal movement during each day between the 1st and 31st of March, as follows. For each day (starting at 17:00 and ending at 16:59 next day), we first simulated the presence of a main resting period with a probability equal to 0.85, its starting time m being randomly drawn between 8:00 and 15:00. The duration (in hours) of this resting period was equal to 15-$m + e$, with e a residual randomly drawn from an Gaussian distribution $\mathcal{N}(0, 1)$, and truncated so that this resting period never ends after 16:59. We then randomly placed patch-level movements during the night between 17:00 and 08:00. We simulated the start time of these patch-level movements by simulating a Poisson process with constant intensity ensuring the presence of 0.66 patches per night on average, with a duration randomly drawn between 0h and 5h. Finally, we placed resting patches in the remaining periods (except between 6:00 and 8:00, when all deer are considered active). We simulated the start time of these resting patches by simulating a Poisson process with constant intensity ensuring the presence of 0.33

patches per night on average, with a duration also randomly drawn between 0h and 5h. Between-patch movements were simulated in the remaining periods.

When the animal switched from one movement type to another (e.g., from between-patches to patch-level, from patch-level to between-patch, or from resting to between-patch), a new attraction point was randomly drawn from the simulated set. When the animal initiated a resting period, it stopped moving immediately and remained stationary until the period ended. An example of simulated movements is given in Fig. 2A.

To satisfy the assumptions underlying the estimation methods, we randomly placed camera traps on the study area (see next sections), and simulated for each trap a motion sensor (i.e., camera traps triggered by the presence of animals, taking at most one picture per second). We defined a detection zone for each trap consisting of a 20 metres circular sector with an angle of 10 degrees. We chose this angle based on Rowcliffe et al. (2008), but the results of the simulations were not affected by this choice (see section S5.5 of Appendix S1 for a set of simulations with an angle of 42 degrees). When the movement of animals crossed the detection zone, we simulated imperfect detection by the sensors (Fig. 2B). We simulated a detection probability decreasing with the distance to the camera trap, and depending on the habitat type where the trap was located. Three habitat types are present in our area: (i) Coppice (76% of the study area), (ii) Open habitat (6% of the study area), (iii) Regeneration (18% of the study area). In Coppice and Open habitat types, we chose the parameters of the detection probability to ensure that the detection probability was equal to 0.99 at 5 metres from the trap and to 0.01 at 18 metres from the trap (calibrated visually from the results of Howe et al., 2017). We simulated the presence of trees obscuring the view in the Coppice habitat type (see Appendix S1 for more details on the distribution of tree diameters). In the Regeneration habitat type, we did not simulate explicitly the presence of such obstacles, but we subjectively chose parameters ensuring a detection probability of 0.99 at 0.5 metres and 0.01 at 3 metres. Finally, we

supposed that an animal resting in the detection zone could not be detected by the sensors. More details on the parameters of the detection process are given in Appendix S1.

Three types of simulations

Roe deer population, no habitat selection

We simulated a simple population dynamics process. We used the data collected on the Chizé study area for the last 45 years as a broad reference for key demographic parameters of a roe deer population (Gaillard et al., 1992, 1993, 1997, and subsequent updates fitted every year to field data). While not directly adopting published estimates, we fine-tuned these parameters to ensure a population decrease over time. Thus, we established an initial population size of 300 roe deer with a balanced sex ratio. Each year, 90% of females were assumed to reproduce, with an average of 1.7 fawns per reproducing female. To facilitate this population decline, we simulated a small survival probability for both the fawns (set at 0.3) and adults (set at 0.7). Though these probabilities were smaller than the values reported by Gaillard et al. (1993) in this area, such probabilities are not unrealistic and could be supposed to result from a high hunting pressure. This indeed resulted in a gradual population decline from 300 animals in Year 1 to 239 animals in Year 5 (see Appendix S1 for exact numbers of animals simulated every year).

We simulated an influence of the decreasing population density on animals' home-range by gradually increasing mean home-range size over time. Kjellander et al. (2004) indeed observed this negative correlation between home-range size and population density in two populations. In reality this relationship can be complex (see discussion), but our aim here was to assess the effect of the opposite effects of the density decline and increasing home-range size on the number of detections by the traps. More precisely, we gradually increased the variance of the OUf process controlling for the between-patch movements. We also varied the list of sets of attraction points used to define the patches, considering only the 19 "small" sets with less than 10 attraction points during the first year, and

progressively adding an increasingly larger sample of the 6 "large" sets with more than 10 attraction points in year 2 to 5. This led to a progressive increase of the home-range size, from an average of 13.1 ha during year 1 (SD = 4.4 ha) to 25.8 ha during year 5 (SD = 12.9 ha). Note that this increase in home-range size also affected the average movement speed of the animals, which may be important given that REM estimators require the knowledge of average speed.

We simulated the movements of all animals of the population during the month of March for every year of the 5-year period. This month was chosen because it coincides with common roe deer monitoring practices and a period of relative stability: it occurs after reproduction (when animals are no longer territorial) and the hunting season, yet before budburst and leaf unfolding, thereby maximizing detection probability. To simulate camera trap monitoring, we randomly placed either 100 or 25 camera traps over the study area, corresponding to a density of approximately 4 traps/km^2 (i.e. $\approx$ one trap per roe-deer home range in average) and 1 trap/km^2 respectively. We then used the REM and IS to estimate the population size from the data collected by these traps (see below). For each density of camera traps (4 or 1/km^2), we carried out 1000 simulations of a camera trap monitoring.

Roe deer population, selection of paths neighborhood

The previous simulations did not account for habitat selection by the target species. In practice, researchers often use their knowledge of habitat use by the species to enhance their monitoring design. This can involve stratification, where pre-specified proportions of camera traps are placed in the different habitats, with overall density calculated as a weighted average of the habitat densities (Rowcliffe et al., 2008). Alternatively, some studies abandon their aim to obtain unbiased population size estimates to improve the precision of unbiased trends estimates. To achieve this, they maximize detection numbers by deploying camera traps only in highly selected habitats or in locations with high

detection probabilities (e.g., Open habitat), assuming a constant bias in size estimates. We assessed these two strategies with a new set of simulations, by simulating a strong habitat selection by the roe deer. We limited these simulations to a trap density of 4 traps/km^2 (100 traps).

We simulated a strong selection of the human paths and roads by the roe deer in our study area. This specific selection of linear features by the roe deer is not expected in reality from a biological point of view, as such features are generally found at the home-range periphery (Seigle-Ferrand et al., 2021). However, this artificial scenario allows us to illustrate the ideal situation where the camera traps are placed in habitats with both high target species abundance and maximum detection probability. In addition, this approach allows us to generalize the results to other species using intensively linear structures, such as large predators (Dickie et al., 2019).

We defined "paths neighborhood" as the 20-metres buffer around each human path or road present in our study area. We simulated a selection of this habitat type by the roe deer: we first selected the location of the home-range centroid in the northern part with a probability of 0.64, as before. However, for this set of simulations, we ensured that: (i) the centroid was located in the paths neighborhood, (ii) it was located at more than 600 m from the border of the study area (to make sure that all the movements were located within the area). Between 3 and 10 attraction points were randomly selected at distances ranging from 100m to 300m from this centroid, making sure that all these points were located within the path neighborhood. We then carried out again the simulations described in the previous section, using these randomly generated attraction points instead of a randomly selected set of attraction points as before. As for the previous set of simulations, we varied the parameter σ^2 of Ornstein-Uhlenbeck processes to simulate an increase in home-range size across years (see Appendix S1).

We then simulated two types of camera trap monitoring, corresponding to the two strategies described previously. In the first simulation type, we assessed the impact of

placing all camera traps within highly selected habitat, specifically by randomly distributing them in the paths neighborhood.

In the second type of simulations, we evaluated the impact of stratified sampling on the precision of population size estimates. We simulated various stratified sampling designs, allocating 5% to 95% of the 100 traps to path neighborhoods in 5% increments. In practice, we did not simulate a single study with X% of traps in the path neighborhoods. Instead, we simulated two separate studies: one with all 100 traps placed in path neighborhoods and another with all 100 traps placed outside of path neighborhoods. To simulate stratified sampling, we combined the detection data from these two scenarios by randomly selecting the detections from X% of the traps from the first study (all traps in path neighborhoods) and the detections from 100-X% of the traps from the second study (all traps outside path neighborhoods). This allowed us to assess the impact of different proportions of traps in path neighborhoods on population size estimates without directly simulating a stratified sampling design within the population itself (which was less computer intensive). Although the animals simulated in the two scenarios (100% and 0% in paths neighborhood) are not the same, we showed in Appendix S1 that the results obtained with this approach do not differ from an approach where we simulated an actual stratified monitoring of the population where all 100 traps study the same animals. Note that we assessed stratification for the estimation of population size during one year only (i.e., no assessment for population trend estimation).

We simulated each strategy type 500 times.

"Red deer" population, no habitat selection

Finally, we aimed to assess the effect of the species home-range size on the results. To do so, we considered an animal with a home-range size similar to that of the red deer (*Cervus elaphus*). Although the simulated animal remains the same as before (e.g. same activity rhythm), with the only difference being a significantly larger home range, we will refer to

this animal as the "red deer" in the following. We used the same movement algorithm as for the roe deer, with the following differences in parameterization: (i) we increased strongly the value of the variance of the between-patch and patch-level movement, (ii) the attraction points are randomly drawn in a rectangular box of 4 kilometres wide centred on the home range centroid. We did not simulate a home-range size varying with population decline over the 5 years. The simulated home-ranges covered 469 ha on average (interquartile range: 383 to 548 ha).

As for the roe deer, we simulated a population size of 300 red deer. This represents a high but not unrealistic density for the species (Borowik and Jwdrzejewska, 2018). We again used published estimates as a broad reference to derive realistic demographic parameters (Bonenfant et al., 2002; Borowik and Jwdrzejewska, 2018). These were fine-tuned ensure a declining population while allowing for comparison with the roe deer results. Specifically, we assumed a sex-ratio of 0.5, an adult annual survival of 0.76, and a reproduction equal to 0.5 fawns per female. The simulated number of red deer was equal to 240 during the last year, corresponding to a 20% decrease in 5 years.

We then placed randomly either 4 traps/km^2 or 1 trap/km^2 over the study area. For each number of traps, we simulated 1000 times the camera trap monitoring.

Population size estimates

For each simulation of each simulation set, we estimated the population size using two methods, REM and IS. To use the REM population size estimator, we need to consider the total number Q of animal-trap encounters. The estimator is:

$$\hat{N}_{\text{rem}} = \frac{S \times Q \times \pi}{A \times v \times r \times (2 + \theta)} \tag{1}$$

With $\hat{N}$ the population size estimate, S the study surface area, A the the cumulated activation duration of the traps, v the mean travel speed of the animals, and r, θ the depth

and angle of the detection zone. Note that one of the biggest difficulties with the REM is that the mean travel speed of the animals is to be estimated, which can be an important source of imprecision of the population size estimation. In our simulations, we have considered that this mean speed is known. Although this will never be the case in practice, our aim was not to devise means to estimate travel speed.

To use the IS population size estimator, we needed to reshape our data. We discretized our study period (the month of March of every year during five years) into one-second intervals. We define "capture occasions" as J discrete moments marking the start of these intervals. For each capture occasion and each animal-camera trap pair, we determined whether a detection occurred (i.e., if the simulated motion sensor of the camera had detected the animal at that time). For each trap i and each capture occasion j, we define a new variable n_{ij} corresponding to the number of animal-trap associations (number of animals present in the detection zone at that time and detected by the trap). Let s_i be the surface area of the detection zone of the camera trap i. The IS population size estimator is:

$$\hat{N}_{\text{IS}} = S \cdot \frac{1}{J} \cdot \frac{1}{M} \sum_{j=1}^{J} \sum_{i=1}^{M} \frac{n_{ij}}{s_i} \tag{2}$$

where M is the number of traps placed in the area.

The two estimation methods were applied each with three modalities: (i) we used the above estimators without accounting for the limited detectability of animals due to imperfect sensors, lack of visibility or activity rhythm (hereafter, these estimators are simply called REM and IS), (ii) we accounted for the limited visibility in the detection zones by modifying these estimators (hereafter called REM_d and IS_d, see below), (ii) we accounted for both this limited visibility and the reduced detectability during resting periods (hereafter called REM_da and IS_da). For the REM estimator, the mean travel speed was computed exactly from the simulated movements, using all data for the REM and REM_d, and using only data collected during active periods for the REM_da.

To account for the imperfect visibility in the detection zone in the REM estimator, we

replaced Q in equation 1 by $Q/\bar{p}$, where $\bar{p}$ is the proportion of all encounters that were detected by the traps. This average detection probability of encounters was estimated from the simulated data, where we knew the exact times when animals crossed trap detection zones. To account for this imperfect detectability of animals in the detection zone in the IS estimator, we replaced s_i by $s_i \times \bar{d}$ in equation 2 where $\bar{d}$ is the mean detection probability of associations. This average detection probability of associations was also estimated from simulated data, where we knew the exact detection probability for all traps (as in fig. 2(B)). Finally, to account for the limited detectability of animals in the detection zone during resting, we changed our study period to remove all the data collected between 8:00 and 17:00, when the main resting period occurs.

For each estimator and each estimation modality, we estimated the population size for each year of the 5 years period, as well as the change rate: $\mathrm{CR} = (N_5 - N_1)/N_1$. We also calculated a mean estimated trend over the 5-year period:

$$\hat{\lambda} = \exp\left\{\frac{\mathrm{Cov}(\log \hat{N}_t, t)}{\mathrm{Var}(t)}\right\} - 1$$

where t is the year and $\hat{N}_t$ the estimated population size during year t. This parameter $\hat{\lambda}$ estimates the proportion of the population disappearing in one year.

When the simulations implied a stratified sample, we calculated one population size estimate for each strata and summed the two estimates. We used the bootstrap to estimate the variances and 90% confidence intervals on population size, change rate and trend estimates, by resampling for each estimation 1000 times with replacement the camera traps and recomputing the estimates to obtain a distribution of 1000 bootstrap estimates. When the simulations implied stratified samples, we bootstrapped the two strata separately.

In total, all these simulations required $\approx$ 20 days of calculation on a Dell T5610 workstation with a processor Intel(R) Xeon(R) CPU E54-2650 (2.6GHz).

Results

Simulating roe deer without habitat selection

We present the results of the simulations in Tables 1 (4 traps/km^2) and 2 (1 trap/km^2). In both cases, it is clear that the two estimators strongly underestimate the population size when the imperfect visibility in the detection zone is not accounted for. The IS estimator showed a far greater bias, underestimating by approximately 80% versus about 35% for the REM. Accounting for this imperfect visibility leads to an unbiased estimate of the population size with the REM, but IS still results in a biased estimate ($\approx$ 20%). Accounting for the limited detectability of the animals in the detection zone when they rest results in an unbiased estimate for both IS and REM. The bootstrap allowed us to correctly estimate the standard error of the sampling distribution for all estimates. Across the 1000 simulations, the trends and change rate were, on average, correctly estimated for all modalities and methods, although considerable variability existed between the simulations.

With 4 traps/km^2 on the study area, the population size estimation was rather imprecise (with a coefficient of variation of about 15% to 20%, depending on the method). A population size decrease was correctly identified in more than 80% (up to 91%) of the simulations with all methods; however, this decrease was significant only in 1/4 to 1/3 of the simulations, depending on the estimation method.

With 1 trap/km^2 on the study area, the population size estimation was even more imprecise (with a coefficient of variation of about 30% to 40%). A population size decrease was estimated correctly in more than 2/3 (up to 74%) of the cases, but this decrease was significant in only 17% of the simulations).

Simulating roe deer with habitat selection

When we simulated habitat selection and placed all the camera traps in the most selected habitat type, the population decrease was overestimated (Table 3). Indeed, the estimated population decline was approximately 8% per year, leading to a 28% decrease in year 5 (i.e., $1 - (1 - 0.08)^4 = 0.28$), instead of the simulated 20% decline (corresponding to a yearly decline of 5.5%).

Using a stratified sample allowed an unbiased population size estimation. The highest precision of the estimation was obtained when half of the traps were placed in the paths neighborhood and half out of this habitat (Fig. 3). However, this stratified sampling did not improve noticeably over a simple random sampling (the smallest coefficients of variation on this graph were similar to those obtained in Table 1).

Simulating a red deer population

The simulations of a red deer population led to the same conclusions regarding the bias and precision of population size estimates: accounting for imperfect visibility in the detection zone led to less biased estimates by the REM and the IS, and accounting for the reduced detectability of resting animals by sensors led to unbiased estimates for the IS. The precision of population size estimates was comparable to that obtained for roe deer, for both 4 traps/km^2 (Table 4) and 1 trap/km^2 (Table 5). However, the trend and change rate estimations were much more precise. With 4 traps/km^2, the simulated decrease was nearly always identified, and was significant in more than 95% of the cases for the REM, and in more than 50% (up to 76%) of the cases for the IS. With 1 trap/km^2, the decrease was also frequently identified in most cases with the REM, and in more than 80% of the cases for the IS. However, the decrease reached statistical significance in only a minority of cases – from 33% (IS) to 66% (REM) of the cases.

We also compared various descriptive statistics between the roe deer and the red deer population (Table 6). The mean number of encounters with red deer was more than twice

that of roe deer. However, the mean speed of red deer was also more than twice bigger than that of roe deer, so that the resulting number of animal-trap associations (and its standard deviation) was similar for the two species. As a result, the population size estimates were comparable between the two populations, whether estimated with REM or by IS. However, since the home-range size was much larger for the red deer than for the roe deer (36 times larger during year 1), the average individual red deer visited 7 times more traps than the average individual roe deer. As a result, each camera trap, on average, detected 7 times more red deer individuals than roe deer individuals. Therefore, when a red deer died between two years, the number of encounters and associations decreased in a larger number of traps than for the roe deer (and conversely when a new animal was born). As a result, by bootstrapping the camera traps to calculate the standard deviation for the trends, it was much easier to detect red deer population changes than roe deer population changes.

Discussion

We have simulated different settings of camera trap monitoring of a roe deer population. Our simulations revealed the importance of accounting for imperfect visibility in the detection zone to estimate the population size correctly with the REM method and even more with the IS method. Moreover, the limited detectability of animals due to their activity rhythm needed to be considered, but exclusively for the IS method. This was less important for the REM, as long as the mean speed was correctly estimated by including inactivity periods. Although the population trend or the change rate were accurately estimated, even without accounting for imperfect visibility or activity rhythm (Table 1), the estimates were very imprecise and often not significantly different from zero. With 1 camera trap/km^2, which is already at the upper end of the density of camera traps typically deployed for this species (e.g. Marcon et al., 2019; Gaudiano et al., 2021; Henrich

et al., 2022; Palencia et al., 2022), the roe deer population size and trend estimates were so imprecise that they were virtually useless (Table 2). When we simulated animals with a much larger home range, the trend estimates were much more precise, even with only 1 trap/km^2. We also showed that placing the traps preferentially in the habitat selected by the species led to a strong overestimate of the population decrease. Finally, we showed that using a stratified sampling did not improve the precision of population size estimation compared to random sampling.

Generalizing our findings to other methods

We used the REM and IS to estimate the population size of the roe deer and red deer populations. We did not compare the two methods to determine which one was the more interesting for the monitoring. Such a comparison would be difficult, as the two methods do not require the same elements to be used. Thus, our results seem to indicate that the two methods give comparable results, though the REM seems more precise than the IS in our simulations. However, as Nakashima (2022) noted, the mean movement speed, which we supposed known in our simulations, is never known in practical studies and has to be estimated. The uncertainty of this parameter estimation results in a larger uncertainty of the population size estimates, so that comparing IS and REM is not fair without accounting for the speed estimation. There are numerous other methods available to estimate the population size based on camera trap data collected on unmarked populations (Nakashima et al., 2017; Moeller et al., 2018), and we chose IS and REM because they were the most easily automated (easily computed estimator that does not rely on the complex fit of a model) and because they belonged to the two main families of estimation methods: methods relying on the encounters and methods relying on associations. We think that our simulation results, that are similar for REM and IS, also generalize to other methods such as camera traps distance sampling, space-to-event or time-to-event models (Howe et al., 2017; Moeller et al., 2018; Calenge, 2025).

Biases and challenges of monitoring protocols

Our results are consistent with previous research highlighting the importance of accounting for the imperfect visibility in the detection zone to obtain unbiased population size estimates (Moeller et al., 2018, 2023). While we assumed perfect knowledge of detection probabilities in our simulations, real-world applications require estimating these probabilities, which can introduce additional uncertainty into population size estimates. Accounting for this imperfect detectability of animals in the detection zones with methods relying on detection is basically the rationale behind the camera-trap distance sampling (Howe et al., 2017). Thus, IS without accounting for detectability is very similar to camera-trap distance sampling where the detection probability is set equal to 1.

In our study, the roe deer population was characterized by a home-range size increasing with time, as a result of the decreasing animal density. This correlation can occur under various ecological conditions. For instance, in the hypothetical case where reduced habitat productivity (e.g., caused by shifts in land management practices) triggers a population decline due to diminished foraging resources, the habitat productivity hypothesis predicts that resource scarcity should also drive an increase in home-range sizes, as individuals compensate for limited resources (Harestad and Bunnel, 1979). Alternatively, this correlation might emerge from density-dependent behavioral mechanisms: declining populations could reduce competition among males, potentially allowing for larger individual territories. Such an inverse relationship between male home-range size and density has been identified in the roe deer by Vincent et al. (1995). In this study, we simulated a negative correlation between home-range size and population, but it is noteworthy that different conditions may lead to a positive correlation, e.g. under habitat productivity hypothesis. For example, if population reductions stem from non-habitat factors (e.g., hunting pressure), lower densities could increase resource availability per capita, thereby shrinking home ranges. Regardless of the underlying mechanism, and whatever their sign, such correlations do exist in nature, and may bias density estimation

with the REM when the increase in home-range size is also correlated with increased mean animal travel speed: in our simulations, the mean speed was 30% smaller in year 1 than in year 5. As the population size estimator is inversely related to this mean speed, using a single value of mean speed for all years, as commonly done in studies using REM, would result in a substantially biased estimation (e.g., using the mean speed of year 1 for all years in equation 1 would result to a 30% underestimation in population size during year 5).

Accounting for activity patterns had a minimal impact on REM population size estimates. The random camera placement meant resting areas were sampled as frequently as active ones. While resting animals are undetectable by motion sensors, their entry and exit from a trap's detection zone, which requires movement, allow encounter detection. Therefore, resting periods within encounters did not affect REM results. On the other hand, since association-based methods strongly rely on the detection of animals at any moment of the encounters, the presence of a resting period during an encounter may lead to a large number of associations missed by a motion-triggered sensor, which explains why association-based methods are more sensitive to activity patterns. Avoiding to include the monitoring periods during which a substantial fraction of the animals are resting allows to remove this small bias, which is also consistent with the findings of previous authors (Howe et al., 2017). This is the simplest approach to account for the activity rhythm of animals, and although other approaches are possible (e.g., by estimating the proportion of the day during which the animal is active and by modifying the duration of the study period in the equations, Nakashima et al., 2017), our approach led to unbiased population size estimates.

Our results raise the question of whether motion-sensors or time-lapse programming of camera traps are preferable for camera trap studies. Association-based methods require time-lapse data, which can be obtained by direct time-lapse programming or post-processing of motion-triggered trap data. Direct time-lapse programming eliminates

sensor sensitivity bias, but image analysis, often AI-assisted (Rigoudy et al., 2023), may still introduce detectability issues related to distance and visibility. Nevertheless, contrary to motion sensors, direct time-lapse programming is not affected by the activity of the animal and detects both active and resting animals equally. However, the short time-lapses needed for association-based methods (Howe et al., 2017) raise storage challenges: trap's memory fills up quickly. Therefore, direct time-lapse programming might not be adequate with association-based methods.

The fact that it was not necessary to account for the activity rhythm of animals and imperfect visibility in the detection zones in our trend estimate is probably a result of our simulation design. Indeed, as long as the simulated detection probability and activity rhythms of animals were the same across years, the resulting bias in the population size estimate was constant, allowing for unbiased estimation of the population trends. However, we do not expect this result to hold if the detectability in the detection zones or the activity rhythm changes across years. For example, the encroachment of shrubs into the study area would lead to an average detection probability decreasing with time. Considering constant detection, or not considering detection at all, would result in an increasing underestimation of population size with time and, consequently in our example of declining population, in an overestimation of the decreasing trend. Not accounting for the activity rhythm or the imperfect detection in trend estimation is only possible under the assumption that these phenomena do not vary with time.

This variation of animal behaviour across years does explain our overestimation of the decline when the traps are placed only in highly-selected habitats. Despite the intuitive aim of maximising detections by positioning all traps in the preferred path neighborhood, this placement led to an overestimation of the decreasing trend (simulated 20% decline vs. estimated 28% over 5 years). This bias stemmed from a simulated change in space use over time: as home-range size increased in later years, individuals spent more time travelling between selected patches, and consequently less time in paths neighborhood in

year 5 than in year 1 (Fig. 4). This between-year variability of the mean proportion of the population located in the paths neighborhood at a given moment directly resulted in the overestimation of the population decrease. Appendix S1 demonstrates mathematically that combining the actual population decrease with this decrease in the proportion of the population in the paths neighborhood results in an annual decrease of 8% of the number of encounters/associations in this habitat. This finding has important consequences for camera trap monitoring, especially given that (i) placing camera traps in good habitats is a common practice to maximize the number of animals detections in population monitoring (e.g., Engeman, 2005; Bengsen et al., 2011); (ii) there are compelling reasons to expect space use to vary considerably and systematically from one year to the next (e.g., Uboni et al., 2015). Thus the common practice of placing camera traps in highly selected habitats carries a high risk of bias in trend estimation.

While altering the sampling strategy could potentially enhance estimate precision, we found no suitable approach; specifically, stratification did not improve precision compared to simple random sampling. Another common strategy involves placing camera traps at the nodes of a regular grid, thereby ensuring a good spatial coverage of the population. We did not consider this grid-based strategy, as it would have yielded results similar to random sampling: given that our simulation design generated a random distribution of home ranges across the study area, the spatial relationship between animals and traps would have been equally random for both grid-based and simple random sampling. The estimates would therefore have been equivalent. Furthermore, density estimation theory assumes random trap placement (e.g. Rowcliffe et al., 2008), making grid-based sampling potentially unsuitable.

Results under idealized conditions

Several aspects of our simulations were oversimplistic: our simulated animals corresponded to a point moving in a 2D space, and not to a volume moving in a 3D space. This

simplification may affect some of our results. For example, when the point representing the animal was located behind a tree, it was supposed to be completely hidden by the tree, whereas in reality animals can be detected by traps when they are located behind small trees. We think that this did not affect strongly our results, as we simulated the presence of trees only for the Coppice habitat type (which represents 76% of the study area), and always at a low density (see Appendix S1 for details): there was in average 0.37 trees simulated in the detection zone of a camera trap located in the Coppice habitat. Simulations showed that the trees obscured in average only 1.2% of the detection zone of a trap in the Coppice habitat, and these trees had more chance to be located far from the traps, i.e., where the detection probability is already low, since this is where the area of the detection zone is the largest.

More generally, simplifying assumptions in our simulations led to an overestimation of precision in our results: our camera traps did not deteriorate with time. We did not simulate any camera trap effect on the detectability of the encounters/associations. Although our simulated animals were characterized by a variable home range size, they all had the same activity rhythm. There were no differences between male and female, or young and adults. Animals were not gregarious (simulating gregarious animals would have led to a greater variance of the encounter rate across camera traps). In other words, it is expected that the uncertainty characterizing the population size and trends estimates in actual studies will be much more important than those obtained in our simulations. And yet our results concerning the roe deer show that the estimation of population size and trends are very imprecise. Even with 4 camera traps/km^2, the coefficient of variation of the population size estimate was about 15 to 20% and increased to 30 to 40% when only 1 trap/km^2 were used. Similar coefficients of variations were obtained in previous studies (e.g., Palencia et al., 2022, obtained CV comprised between 34% to 75% when estimating the population size of various species with the REM, on areas comprised between 1400 to 6600 ha with 7 to 37 camera traps – corresponding to 0.3 to 1.3 camera traps/km^2 –

during periods covering 15 to 138 days). Our study showed that a strong population decrease of 20% in 5 years was not significant in 62% to 75% of the simulations when 4 traps/km^2 were used, and this proportion rose to 82% when a density of only 1 trap/km^2 was used. As our simulations were very optimistic, this proportion is expected to be much smaller in real studies. This shows that the use of camera traps for the monitoring of roe deer population trends is probably of very limited value.

The key role of home-range size

The results obtained for the red deer were more encouraging. Even with only 1 camera trap/km^2, we were able to statistically detect a 20% decrease of the population size in 33% to 68% of the simulations, depending on the methods used. This is still a low sensitivity, given the strong simulated population decrease and the perfect knowledge of some parameters in our simulations. However, these results indicate that camera traps monitoring might not be immediately dismissed for larger species in areas of size similar to the Chizé forest. An important quantity governing the choice to use or not camera traps for population monitoring is the number of different camera traps that can capture a given animal in a given study area. This metric depends on multiple factors, including the number of traps deployed, the species' home-range size, heterogeneity of space use within the home range, and the size of the study area. For example, considering the red deer in our study, randomly placing 100 camera traps over the 2600 ha study area resulted in a density of approximately 4 traps/km^2, meaning that roughly 18 traps were included within the average 4.5 km^2 home-range. Because the simulated red deer home-range use was highly heterogeneous, with activity concentrated around a limited number of attraction points (see Appendix S1 for an illustration), the actual number of traps detecting a given red deer was considerably reduced, averaging 3.5 traps per animal (Table 4). Consequently, the death of a red deer between two years is detected by an average of 3.5 traps, resulting in a clear decrease in the number of encounters/associations detected by

the traps. This explains the effectiveness of camera trap monitoring for this species under these conditions. In contrast, with a larger study area of 20000 ha and the same 100 traps, the trap density would decrease to 0.5 traps/km^2. This would result in approximately $0.5 \times 3.5/4 = 0.44$ different traps encountered by a given red deer in average, similar to the value obtained for the roe deer in our simulations (Table 4). Indeed, for roe deer, with only 0.45 traps visited per animal in Chizé, most individuals remain undetected, resulting in low power to statistically detect population declines.

Management implications

While this study provided unbiased estimates of population sizes, it also revealed important limitations for monitoring roe deer populations with camera traps: low precision and a high susceptibility to spatiotemporal variations in animal behavior. Although the results for the red deer were more encouraging, we must keep in mind that population units for this species are generally much larger than 2600 ha (in France, typical red deer management units used by hunters associations often exceed 10 000 ha; Maryline Pellerin, com. pers.). Consequently, the number of camera traps per red-deer home range in a typical wildlife management context would likely be too low, leading to low-precision estimates. The gregarious behaviour of this species could further exacerbate this imprecision. Thus, even if camera trap monitoring might be promising for scientific studies in small areas, its practical ability for day-to-day population monitoring by wildlife managers remain questionable, even for the red deer.

In fact, we advise the reader to proceed to simulations to determine whether or not camera traps are a suitable choice to design a monitoring a given population of a given species, and to proceed to the best adaptations. Our R package `simCTChize` can be useful to carry out such simulations. Appendix S1, also available as a vignette of the package, contains a tutorial explaining how it can be used to reach this aim.

Acknowledgements

We warmly thank our colleagues of the French biodiversity management organisation (*Office français de la biodiversité*), and in particular the members of the MAS network (*Mathématique appliquée et statistiques*), who provided feedback and constructive criticisms on these results.

References

Bengsen, A.J., L.K.P. Leung, S.J. Lapidge, and I.J. Gordon. 2011. "Using a general index approach to analyze cameratrap abundance indices." *The Journal of Wildlife Management* 75: 1222–1227.

Blackwell, P.G. 1997. "Random diffusion models for animal movement." *Ecological Modelling* 100: 87–102.

Bonenfant, C., J.M. Gaillard, F. Klein, and A. Loison. 2002. "Sex-and age-dependent effects of population density on life history traits of red deer *Cervus elaphus* in a temperate forest." *Ecography* 25: 446–458.

Borowik, T., and B. Jwdrzejewska. 2018. "Europe-wide consistency in density-dependence of red deer (*Cervus elaphus*) fertility." *Mammalian Biology* 89: 95–99.

Burton, A.C., E. Neilson, D. Moreira, A. Ladle, R. Steenweg, J.T. Fisher, E. Bayne, and S. Boutin. 2015. "Wildlife camera trapping: a review and recommendations for linking surveys to ecological processes." *Journal of Applied Ecology* 52: 675–685.

Calenge, C. 2025. "Camera trap monitoring of unmarked animals: a map of the relationships between population size estimators." *bioRxiv* in prep.: 1–11.

Campos-Candela, A., M. Palmer, S. Balle, and J. Alós. 2018. "A camera-based method for estimating absolute density in animals displaying home range behaviour." *Journal of Animal Ecology* 87: 825–837.

Caravaggi, A., M. Zaccaroni, F. Riga, S.C. Schai-Braun, J.T.A. Dick, W.I. Montgomery, and N. Reid. 2016. "An invasive-native mammalian species replacement process captured by camera trap survey random encounter models." *Remote Sensing in Ecology and Conservation* 2: 45–58.

Corlatti, L., S. Sivieri, B. Sudolska, S. Giacomelli, and L. Pedrotti. 2020. "A field test of unconventional camera trap distance sampling to estimate abundance of marmot populations." *Wildlife Biology* 2020: 1–11.

Dickie, M., S.R. McNay, G.D. Sutherland, M. Cody, and T. Avgar. 2019. "Corridors or risk? Movement along, and use of, linear features varies predictably among large mammal predator and prey species." *Journal of Animal Ecology* 89: 623–634.

Engeman, R.M. 2005. "Indexing principles and a widely applicable paradigm for indexing animal populations." *Wildlife Research* 32: 203–210.

Fleming, C.H., J.M. Calabrese, T. Mueller, K.A. Olson, P. Leimgruber, and W.F. Fagan. 2014. "From fine-scale foraging to home ranges: a semivariance approach to identifying movement modes across spatiotemporal scales." *The American Naturalist* 183: E154–E167.

Gaillard, J.M., J.M. Boutin, D. Delorme, G. van Laere, P. Duncan, and J.D. Lebreton. 1997. "Early survival in roe deer: causes and consequences of cohort variation in two contrasted populations." *Oecologia* 112: 502–513.

Gaillard, J.M., D. Delorme, J.M. Boutin, G. van Laere, B. Boisaubert, and R. Pradel. 1993. "Roe Deer Survival Patterns: A Comparative Analysis of Contrasting Populations." *The Journal of Animal Ecology* 62: 778.

Gaillard, J.M., A.J. Sempéré, J.M. Boutin, G. Van Laere, and B. Boisaubert. 1992. "Effects of age and body weight on the proportion of females breeding in a population of roe deer (*Capreolus capreolus*)." *Canadian Journal of Zoology* 70: 1541–1545.

Garel, M., C. Bonenfant, J.-L. Hamann, F. Klein, and J.-M. Gaillard. 2010. "Are abundance

indices derived from spotlight counts reliable to monitor red deer populations?." *Wildlife Biology* 16: 77–84.

Gaudiano, L., L. Pucciarelli, and E. Mori. 2021. "Livestock grazing affects movements and activity pattern of Italian roe deer in Southern Italy." *European Journal of Wildlife Research* 67: 1–8.

Gaudry, W., J.M. Gaillard, S. Saïd, C. Bonenfant, A. Mysterud, N. Morellet, and C. Calenge. 2018. "Same habitat composition but different use: evidence of context-dependent habitat selection in roe deer females." *Scientific reports* 8: 5102.

Gilbert, N.A., J.D.J. Clare, J.L. Stenglein, and B. Zuckerberg. 2020. "Abundance estimation of unmarked animals based on camera-trap data." *Conservation Biology* 35: 88–100.

Glen, A.S., S. Cockburn, M. Nichols, J. Ekanayake, and B. Warburton. 2013. "Optimising Camera Traps for Monitoring Small Mammals." *PLoS ONE* 8: e67940.

Guillera-Arroita, G. 2017. "Modelling of species distributions, range dynamics and communities under imperfect detection: advances, challenges and opportunities." *Ecography* 40: 281–295.

Harestad, A.S., and FL Bunnel. 1979. "Home range and body weight–a reevaluation." *Ecology* 60: 389–402.

Henrich, M., F. Hartig, C.F. Dormann, H.S. Kühl, W. Peters, F. Franke, T. Peterka, P. ustr, and M. Heurich. 2022. "Deer Behavior Affects Density Estimates With Camera Traps, but Is Outweighed by Spatial Variability." *Frontiers in Ecology and Evolution* 10: 1–17.

Howe, E.J., S.T. Buckland, M.L. Després-Einspenner, and H.S. Kühl. 2017. "Distance sampling with camera traps." *Methods in Ecology and Evolution* 8: 1558–1565.

Karanth, K.U. 1995. "Estimating tiger Panthera tigris populations from camera-trap data using capture/recapture models." *Biological Conservation* 71: 333–338.

Kjellander, P., A.J.M. Hewison, O. Liberg, J.M. Angibault, E. Bideau, and B. Cargnelutti. 2004. "Experimental evidence for density-dependence of home-range size in roe deer (*Capreolus capreolus* L.): a comparison of two long-term studies." *Oecologia* 139: 478–485.

Marcon, A., D. Battocchio, M. Apollonio, and S. Grignolio. 2019. "Assessing precision and requirements of three methods to estimate roe deer density." *PLOS ONE* 14: e0222349.

Michelot, T., P. Gloaguen, P.G. Blackwell, and M.P. Etienne. 2019. "The Langevin diffusion as a continuous-time model of animal movement and habitat selection." *Methods in Ecology and Evolution* 10: 1894–1907.

Moeller, A.K., P.M. Lukacs, and J.S. Horne. 2018. "Three novel methods to estimate abundance of unmarked animals using remote cameras." *Ecosphere* 9: e02331.

Moeller, A.K., S.J. Waller, N.J. DeCesare, M.C. Chitwood, and P.M. Lukacs. 2023. "Best practices to account for capture probability and viewable area in camera-based abundance estimation." *Remote Sensing in Ecology and Conservation* 9: 152–164.

Morellet, N., J.-M. Gaillard, A.J.M. Hewison, P. Ballon, Y. Boscardin, P. Duncan, F. Klein, and D. Maillard. 2007. "Indicators of ecological change: new tools for managing populations of large herbivores.." *Journal of Applied Ecology* 44: 634–643.

Nakashima, Y. 2022. "Guidelines for evaluating density estimation models for unmarked populations - Santini et al. (2022)." *Basic and Applied Ecology* 65: 109–110.

Nakashima, Y., K. Fukasawa, and H. Samejima. 2017. "Estimating animal density without individual recognition using information derivable exclusively from camera traps." *Journal of Applied Ecology* 55: 735–744.

Palencia, P., P. Barroso, J. Vicente, T.R. Hofmeester, J. Ferreres, and P. Acevedo. 2022. "Random encounter model is a reliable method for estimating population density of multiple species using camera traps." *Remote Sensing in Ecology and Conservation* 8: 670–682.

Palencia, P., J. Vicente, R. C. Soriguer, and P. Acevedo. 2021. "Towards a bestpractices guide for camera trapping: assessing differences among camera trap models and settings under field conditions." *Journal of Zoology* 316: 197–208.

Pellerin, M., A. Bessière, D. Maillard, G. Capron, J.M. Gaillard, J. Michallet, and C. Bonenfant. 2017. "Saving time and money by using diurnal vehicle counts to monitor roe deer abundance." *Wildlife Biology* 2017: 1–10.

Pellerin, M., C. Calenge, S. Saïd, J.M. Gaillard, H. Fritz, P. Duncan, and G. Van Laere. 2010. "Habitat use by female western roe deer (*Capreolus capreolus*): influence of resource availability on habitat selection in two contrasting years." *Canadian Journal of Zoology* 88: 1052–1062.

Pellerin, M., S. Saïd, and J.M. Gaillard. 2008. "Roe deer *Capreolus capreolus* home-range sizes estimated from VHF and GPS data." *Wildlife Biology* 14: 101–110.

Pettorelli, N., J.M. Gaillard, P. Duncan, J.P. Ouellet, and G. Van Laere. 2001. "Population density and small-scale variation in habitat quality affect phenotypic quality in roe deer." *Oecologia* 128: 400–405.

Rigoudy, N., G. Dussert, A. Benyoub, A. Besnard, C. Birck, J. Boyer, Y. Bollet, Y. Bunz, G. Caussimont, E. Chetouane, and S. Chamaille-Jammes. 2023. "The DeepFaune initiative: a collaborative effort towards the automatic identification of European fauna in camera trap images." *European Journal of Wildlife Research* 69: 113–113.

Rovero, F., and A.R. Marshall. 2009. "Camera trapping photographic rate as an index of density in forest ungulates." *Journal of Applied Ecology* 46: 1011–1017.

Rowcliffe, J.M., J. Field, S.T. Turvey, and C. Carbone. 2008. "Estimating animal density using camera traps without the need for individual recognition." *Journal of Applied Ecology* 45: 1228–1236.

Rowcliffe, J.M., R. Kays, B. Kranstauber, C. Carbone, and P.A. Jansen. 2014. "Quantifying

levels of animal activity using camera trap data." *Methods in Ecology and Evolution* 5: 1170–1179.

Saïd, S., J.M. Gaillard, P. Duncan, N. Guillon, N. Guillon, S. Servanty, M. Pellerin, K. Lefeuvre, C. Martin, and G. van Laere. 2005. "Ecological correlates of home-range size in spring–summer for female roe deer (*Capreolus capreolus*) in a deciduous woodland." *Journal of Zoology* 267: 301–308.

Santini, G., M. Abolaffio, F. Ossi, B. Franzetti, F. Cagnacci, and F. Focardi. 2022. "Population assessment without individual identification using camera-traps: A comparison of four methods." *Basic and Applied Ecology* 61: 68–81.

Seigle-Ferrand, J., P. Marchand, N. Morellet, J.M. Gaillard, A.J.M. Hewison, S. Saïd, Y. Chaval, H. Santacreu, A. Loison, G. Yannic, and M. Garel. 2021. "On this side of the fence: Functional responses to linear landscape features shape the home range of large herbivores." *Journal of Animal Ecology* 91: 443–457.

Twining, J.P., C. McFarlane, D. O'Meara, C. O'Reilly, M. Reyne, W.I. Montgomery, S. Helyar, D.G. Tosh, and B.C. Augustine. 2022. "A comparison of density estimation methods for monitoring marked and unmarked animal populations." *Ecosphere* 13: e4165.

Uboni, A., J.A. Vucetich, D.R. Stahler, and D.W. Smith. 2015. "Interannual variability: a crucial component of space use at the territory level." *Ecology* 96: 62–70.

Vincent, J.P., E. Bideau, A.J.M. Hewison, and J.M. Angibault. 1995. "The influence of increasing density on body weight, kid production, home range and winter grouping in roe deer (*Capreolus capreolus*)." *Journal of Zoology* 236: 371–382.

Williams, B.K., J.D. Nichols, and M.J. Conroy. 2002. *Analysis and management of animal populations: modeling, estimation, and decision making*, Academic Press, New York.

Table 1: Results of 1000 simulations of a roe deer population monitored for 5 years using 4 camera traps/km^2.

Method	Param	TrueValue	MeanEst	SE	SEEst	SE.SEEst	Pcov	PDec	PsigD
REM	N1	300	237.31	37.875	38.687	6.215	0.511		
REM	N5	239	181.767	33.792	31.553	6.114	0.444		
REM	λ	-0.0547	-0.063	0.049	0.048	0.007	0.869	0.906	0.364
REM	CR	-0.2033	-0.22	0.165	0.165	0.043	0.859	0.906	0.378
REM_d	N1	300	303.86	45.68	49.51	7.853	0.923		
REM_d	N5	239	232.533	40.045	40.352	7.572	0.882		
REM_d	λ	-0.0547	-0.063	0.049	0.048	0.007	0.867	0.906	0.367
REM_d	CR	-0.2033	-0.22	0.165	0.169	0.042	0.9	0.906	0.327
REM_da	N1	300	303.224	47.154	50.959	8.427	0.928		
REM_da	N5	239	232.706	41.018	41.146	7.83	0.882		
REM_da	λ	-0.0547	-0.062	0.051	0.05	0.007	0.867	0.889	0.344
REM_da	CR	-0.2033	-0.217	0.172	0.176	0.045	0.904	0.891	0.311
IS	N1	300	54.903	9.955	10.084	1.897	0		
IS	N5	239	42.983	8.975	8.3	1.844	0		
IS	λ	-0.0547	-0.058	0.055	0.055	0.008	0.88	0.843	0.289
IS	CR	-0.2033	-0.198	0.195	0.198	0.057	0.87	0.848	0.279
IS_d	N1	300	262.512	47.812	46.688	11.689	0.737		
IS_d	N5	239	205.374	40.169	37.611	9.195	0.682		
IS_d	λ	-0.0547	-0.057	0.056	0.054	0.008	0.884	0.854	0.279
IS_d	CR	-0.2033	-0.197	0.196	0.197	0.056	0.882	0.841	0.276
IS_da	N1	300	298.869	57.784	56.794	15.407	0.881		
IS_da	N5	239	233.97	49.233	45.015	12.228	0.849		
IS_da	λ	-0.0547	-0.057	0.059	0.057	0.009	0.885	0.833	0.272
IS_da	CR	-0.2033	-0.193	0.211	0.214	0.067	0.891	0.834	0.257

Abbreviation: REM, random encounter model; IS, instantaneous sampling; _d, accounting for imperfect visibility; _da, accounting for imperfect visibility and resting periods; N1 and N5, population size during years 1 and 5 respectively; λ, trend over five years; CR = [N5-N1]/N1; TrueValue, simulated value of a parameter; MeanEst, mean of estimated values; SE, standard deviation of estimated values; SEEst, mean of the bootstrap estimates of SE; SE.SEEst, standard deviation of the boostrap esitmates of SE; Pcov, estimated coverage probability of the 90% confidence interval; Pdec, proportion of simulations for which estimated λ or CR is negative; PsigD, proportion of simulations for which this decrease is significant at the 10% level.

Table 2: Results of 1000 simulations of a roe deer population monitored for 5 years using 1 camera trap/km^2.

Method	Param	TrueValue	MeanEst	SE	SEEst	SE.SEEst	Pcov	PDec	PsigD
REM	N1	300	235.668	78.199	72.339	23.699	0.688		
REM	N5	239	181.565	64.232	59.381	21.176	0.638		
REM	λ	-0.0547	-0.057	0.099	0.097	0.026	0.87	0.732	0.186
REM	CR	-0.2033	-0.161	0.383	0.417	0.358	0.871	0.738	0.193
REM_d	N1	300	301.727	93.669	92.96	29.521	0.868		
REM_d	N5	239	232.242	76.207	76.196	26.018	0.864		
REM_d	λ	-0.0547	-0.057	0.099	0.097	0.026	0.872	0.732	0.192
REM_d	CR	-0.2033	-0.161	0.383	0.417	0.289	0.887	0.738	0.161
REM_da	N1	300	301.069	97.229	95.555	31.466	0.871		
REM_da	N5	239	231.893	78.276	77.683	26.871	0.861		
REM_da	λ	-0.0547	-0.056	0.104	0.1	0.027	0.861	0.722	0.187
REM_da	CR	-0.2033	-0.15	0.413	0.436	0.276	0.877	0.734	0.159
IS	N1	300	54.785	20.805	18.818	7.119	0		
IS	N5	239	42.953	16.803	15.415	6.117	0		
IS	λ	-0.0547	-0.053	0.115	0.111	0.034	0.856	0.701	0.159
IS	CR	-0.2033	-0.107	0.503	0.628	0.908	0.848	0.701	0.166
IS_d	N1	300	263.562	97.551	87.342	36.81	0.768		
IS_d	N5	239	204.538	75.535	69.373	28.575	0.745		
IS_d	λ	-0.0547	-0.053	0.113	0.108	0.03	0.851	0.699	0.157
IS_d	CR	-0.2033	-0.119	0.482	0.605	1.06	0.856	0.703	0.167
IS_da	N1	300	301.313	120.668	105.91	50.082	0.816		
IS_da	N5	239	233.349	91.489	83.106	36.841	0.826		
IS_da	λ	-0.0547	-0.051	0.124	0.115	0.033	0.856	0.699	0.147
IS_da	CR	-0.2033	-0.091	0.586	0.813	3.492	0.85	0.688	0.155

Note: We use the same abbrevations as in Table 1

Table 3: Results of 500 simulations of a roe deer population monitored for 5 years using 4 camera traps/km^2, where all animals display a preference for the neighborhood of paths and where all the traps have been placed in this neighborhood.

Method	Param.	MeanEst	SE	SEEst	SE.SEEst	Pcov	PDec	PsigD
REM	-0.0547	-0.08	0.03	0.03	0.00	0.73	1.00	0.87
REM_d	-0.0547	-0.08	0.03	0.03	0.00	0.73	1.00	0.86
REM_da	-0.0547	-0.08	0.03	0.03	0.00	0.75	1.00	0.83
IS	-0.0547	-0.08	0.04	0.04	0.01	0.77	0.99	0.70
IS_d	-0.0547	-0.08	0.04	0.04	0.01	0.79	0.99	0.71
IS_da	-0.0547	-0.08	0.04	0.04	0.01	0.81	0.99	0.69

Note: We use the same abbrevations as in Table 1

Table 4: Results of 500 simulations of a red deer population monitored for 5 years using 4 camera traps/km^2.

Method	Param	TrueValue	MeanEst	SE	SEEst	SE.SEEst	Pcov	PDec	PsigD
REM	N1	300	207.511	40.895	40.456	4.87	0.325		
REM	N5	240	165.729	33.028	32.409	4.006	0.315		
REM	λ	-0.0543	-0.055	0.013	0.012	0.002	0.875	1	0.989
REM	CR	-0.2	-0.2	0.047	0.046	0.009	0.885	1	0.976
REM_d	N1	300	296.257	52.281	57.931	6.602	0.916		
REM_d	N5	240	236.537	41.961	46.383	5.297	0.916		
REM_d	λ	-0.0543	-0.055	0.013	0.012	0.002	0.874	1	0.991
REM_d	CR	-0.2	-0.2	0.047	0.046	0.009	0.937	1	0.993
REM_da	N1	300	296.516	52.561	57.848	6.605	0.921		
REM_da	N5	240	236.556	42.166	46.411	5.377	0.916		
REM_da	λ	-0.0543	-0.055	0.015	0.015	0.003	0.879	1	0.968
REM_da	CR	-0.2	-0.2	0.057	0.054	0.011	0.931	0.999	0.964
IS	N1	300	51.406	10.502	10.236	1.301	0		
IS	N5	240	41.187	8.642	8.3	1.119	0		
IS	λ	-0.0543	-0.054	0.022	0.022	0.005	0.888	0.988	0.761
IS	CR	-0.2	-0.195	0.086	0.084	0.02	0.872	0.982	0.704
IS_d	N1	300	259.127	48.484	47.458	7.392	0.748		
IS_d	N5	240	208.346	39.598	39.027	6.823	0.76		
IS_d	λ	-0.0543	-0.053	0.026	0.026	0.007	0.892	0.974	0.672
IS_d	CR	-0.2	-0.19	0.101	0.099	0.034	0.889	0.959	0.611
IS_da	N1	300	295.255	57.31	55.822	10.413	0.879		
IS_da	N5	240	237.832	47.503	46.435	10.191	0.874		
IS_da	λ	-0.0543	-0.053	0.031	0.03	0.008	0.893	0.957	0.583
IS_da	CR	-0.2	-0.187	0.12	0.117	0.045	0.897	0.936	0.51

Note: We use the same abbrevations as in Table 1

Table 5: Results of 500 simulations of a red deer population monitored for 5 years using 1 camera traps/km^2.

Method	Param	TrueValue	MeanEst	SE	SEEst	SE.SEEst	Pcov	PDec	PsigD
REM	N1	300	210.484	80.766	78.826	19.945	0.655		
REM	N5	240	167.931	65.534	62.97	15.982	0.658		
REM	λ	-0.0543	-0.055	0.028	0.025	0.009	0.835	0.979	0.679
REM	CR	-0.2	-0.197	0.103	0.105	0.058	0.846	0.967	0.63
REM_d	N1	300	299.684	104.803	113.481	27.342	0.902		
REM_d	N5	240	239.059	84.642	90.663	21.937	0.895		
REM_d	λ	-0.0543	-0.055	0.028	0.025	0.01	0.835	0.979	0.673
REM_d	CR	-0.2	-0.197	0.103	0.105	0.059	0.88	0.967	0.645
REM_da	N1	300	299.633	104.979	112.892	27.098	0.902		
REM_da	N5	240	238.704	84.816	90.233	22.085	0.903		
REM_da	λ	-0.0543	-0.055	0.034	0.028	0.01	0.817	0.95	0.582
REM_da	CR	-0.2	-0.194	0.134	0.123	0.069	0.88	0.936	0.561
IS	N1	300	51.964	20.603	19.837	5.205	0		
IS	N5	240	41.302	16.859	15.898	4.35	0		
IS	λ	-0.0543	-0.056	0.05	0.043	0.017	0.828	0.878	0.423
IS	CR	-0.2	-0.185	0.199	0.227	0.348	0.816	0.85	0.376
IS_d	N1	300	260.332	95.011	91.322	25.821	0.823		
IS_d	N5	240	208.851	80.911	74.454	22.685	0.808		
IS_d	λ	-0.0543	-0.055	0.055	0.047	0.018	0.844	0.858	0.365
IS_d	CR	-0.2	-0.178	0.224	0.249	0.382	0.841	0.834	0.34
IS_da	N1	300	295.397	110.777	106.145	33.628	0.862		
IS_da	N5	240	238.746	98.29	87.876	31.69	0.854		
IS_da	λ	-0.0543	-0.054	0.065	0.054	0.02	0.824	0.819	0.328
IS_da	CR	-0.2	-0.164	0.277	0.325	0.726	0.813	0.791	0.289

Note: We use the same abbrevations as in Table 1

Table 6: Mean value (SD in parentheses) of various statistics calculated for each simulation of camera trap monitoring of roe deer and red deer population (300 individuals,100 camera traps).

	Roe Deer	Red Deer
Number of associations	19172 (SD = 3476)	17951 (SD = 3667)
Number of encounters	684 (SD = 101)	1584 (SD = 279)
Travel speed ($m.s^{-1}$)	0.0165 (SD = 0.0001)	0.0387 (SD = 0.0002)
Number of traps visited by an animal	0.459 (SD = 0.056)	3.492 (SD = 0.62)
Number of animals seen by a trap	1.376 (SD = 0.167)	10.475 (SD = 1.86)

Figure legends

Figure 1. Simulation of the movement of a roe deer during a typical day, starting at 17:00 and ending at 16:59 the following day. The sequence 1 – 5 describes the simulation of the activity cycle. The point 6 illustrates the simulation of the movement process itself, zooming on the beginning of the day.

Figure 2. Simulation process used : (A) simulation of the movements of a roe deer using a model combining multiple Ornstein-Uhlenbeck process, including resting patches (green points) within the movement (when the animals stay at the same place without moving at all, (B) simulation of the detection process by a camera trap. The detection zone is modelled as a circular sector with a radius of 20 m and an angle equal to 10 degrees. Detection probability decreases with increasing distance from the trap, represented by varying shades of grey (darker = lower detection probability, and black = no detection at all). We also simulate the presence of trees that may limit the visibility within the detection zone. The movements of the animal simulated on panel (A) are displayed in red on this figure. The camera traps can capture the animals every second. The points correspond to the detections of the animals (more numerous close to the trap).

Figure 3. Precision of the estimation of population size in a monitoring of a roe deer population with 300 individuals with 4 camera traps/km^2, using stratified sampling. The animals display a strong preference for the paths neighborhood on our study area (which represents 38% of the study area), and we vary the proportion of traps in this habitat type. We use two methods to estimate population size, the random encounter model (REM) and the instantaneous sampling (IS). For each method, we estimate the population size: (i) without accounting for imperfect visibility in the detection zones or the limited detectability of the animals in the detection zones during their resting periods (REM and IS), (ii) accounting for imperfect detectability of animals in the detection zones but not for

these resting periods (REM_d, IS_d), (iii) accounting for both imperfect detectability and these resting periods (REM_da and IS_da)

Figure 4. Estimated mean time spent by the roe deer in the paths neighborhood every year, in our simulations of a camera trap monitoring over 5 years. Since the home-range size of the animals increases with time, animals spend less time in average in "good" habitats.

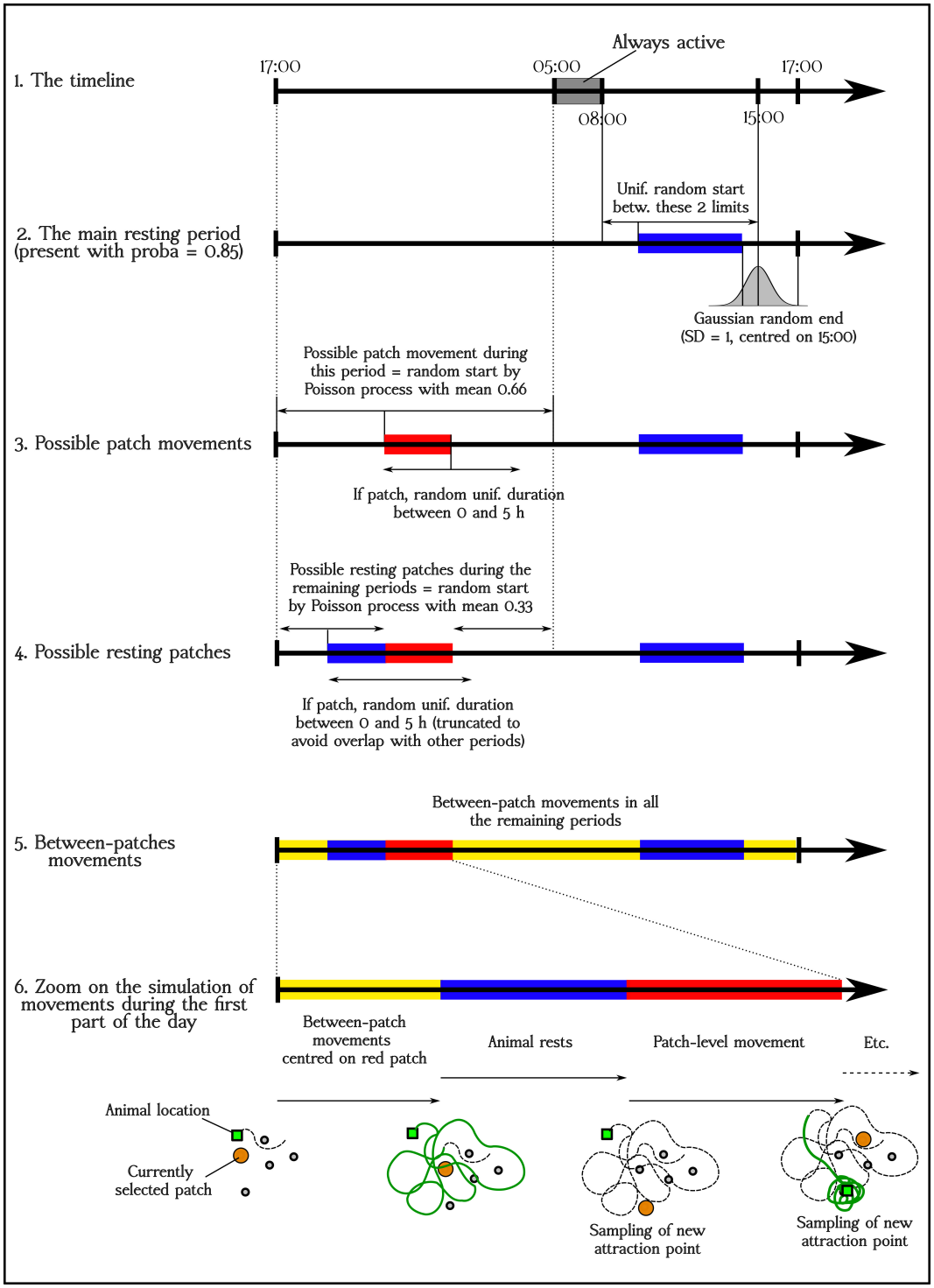
1. The timeline
17:00
05:00
Always active
17:00
08:00
15:00
2. The main resting period
(present with proba = 0.85)
Unif. random start
betw. these 2 limits
Gaussian random end
(SD = 1, centred on 15:00)
3. Possible patch movements
Possible patch movement during
this period = random start by
Poisson process with mean 0.66
If patch, random unif. duration
between 0 and 5 h
4. Possible resting patches
Possible resting patches during the
remaining periods = random start
by Poisson process with mean 0.33
If patch, random unif. duration
between 0 and 5 h (truncated to
avoid overlap with other periods)
5. Between-patches
movements
Between-patch movements in all
the remaining periods
6. Zoom on the simulation of
movements during the first
part of the day
Between-patch
movements
centred on red patch
Animal rests
Patch-level movement
Etc.
Animal location
Currently
selected patch
Sampling of new
attraction point
Sampling of new
attraction point

Figure 1

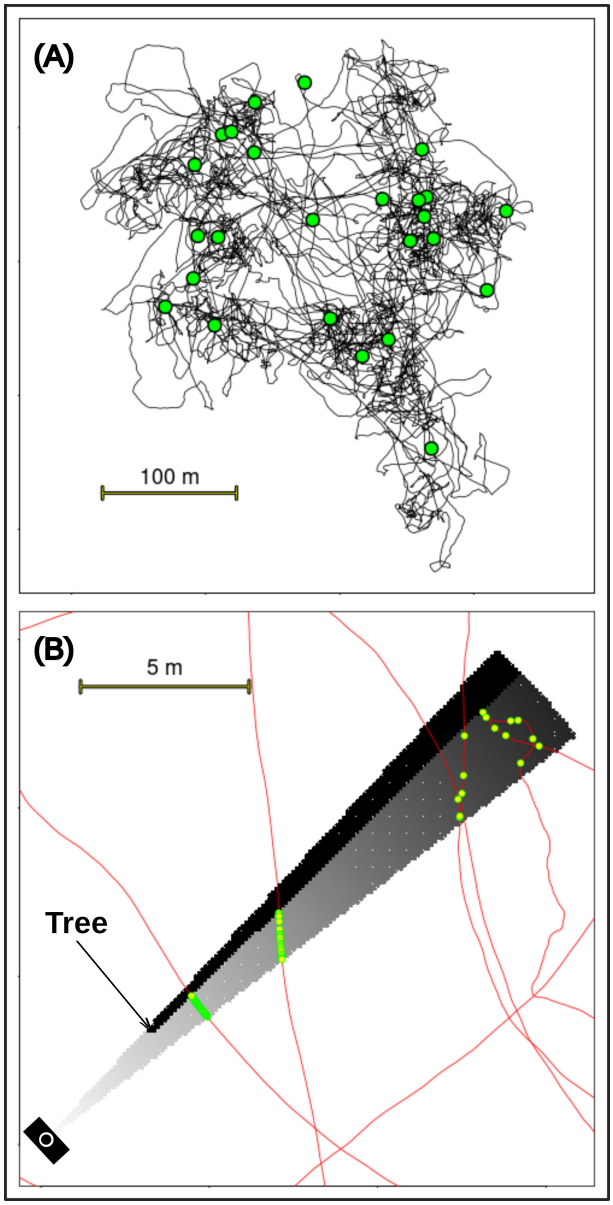

Figure 2

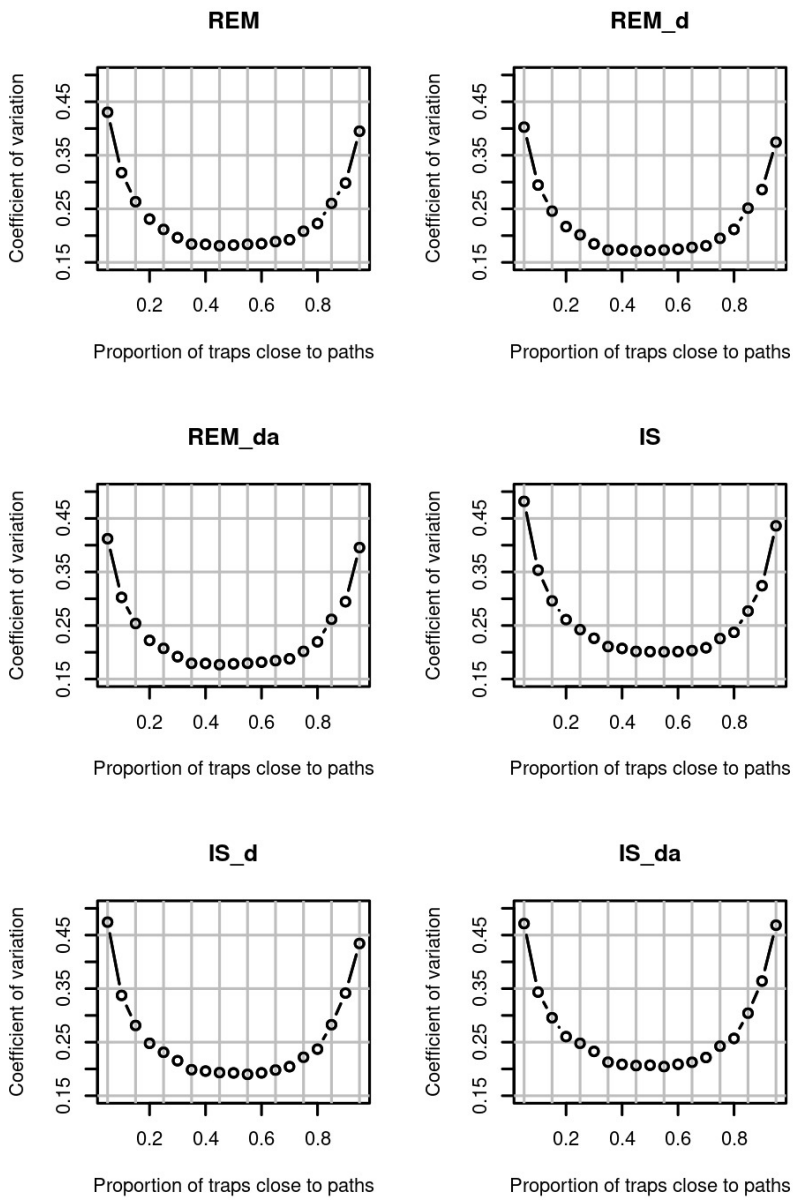
REM
REM_d
REM_da
IS
IS_d
IS_da
Coefficient of variation
0.15
0.25
0.35
0.45
0.2
0.4
0.6
0.8
Proportion of traps close to paths

Figure 3

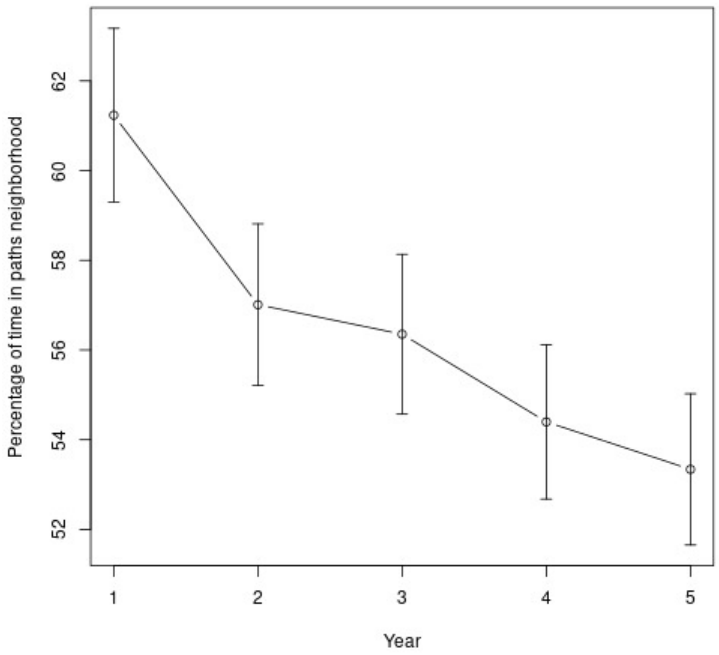
Percentage of time in paths neighborhood
52
54
56
58
60
62
1
2
3
4
5
Year

Figure 4